Electroanalysis

ELECTROANALYSIS
An International Journal Devoted to Electroanalysis, Sensors and Bioelectronic Devices

RESEARCH ARTICLE OPEN ACCESS

Study of the Oxidation Behavior of Tyrosine Using Electrochemistry, Capillary Electrophoresis, and Mass Spectrometry

Seyedehelahe Bagherimetkazini | Frank-Michael Matysik

Faculty of Chemistry and Pharmacy, Institute of Analytical Chemistry, Chemo- and Biosensors, University of Regensburg, Regensburg, Germany

Correspondence: Frank-Michael Matysik (frank-michael.matysik@chemie.uni-regensburg.de)

Received: 22 February 2026 | **Revised:** 9 April 2026 | **Accepted:** 23 April 2026

Keywords: capillary electrophoresis | electrochemistry | mass spectrometry | tyrosine

ABSTRACT

The oxidation behavior of L-tyrosine was studied using a carbon-based screen-printed electrode in ammonium acetate buffer, coupled with an electrochemical flow cell and mass spectrometry via capillary electrophoresis. Cyclic voltammetry and linear sweep voltammetry were employed to investigate the oxidation behavior of this compound. The migration in capillary electrophoresis, mass-to-charge ratios, and isotopic patterns of L-tyrosine's oxidation products were examined. Results indicated that three different diffusive oxidation products could be detected within a potential range of 0–1.3 V. Because measurements are made over a short time, both stable oxidation products and intermediates could be observed. Three main product species were recorded with real-time electrochemistry-mass spectrometry and electrochemistry coupled to capillary electrophoresis-mass spectrometry. The product species 3-nitrotyrisine was identified with the help of an available standard, and the formulas of the other two product species were determined, along with suggestions corresponding to structures.

1 | Introduction

Tyrosine (Tyr) is one of the nonessential amino acids involved in key physiological processes. Several studies have detected Tyr-related oxidation products in serum, eye lens, cerebrospinal fluid, and brain. These findings suggest that increased levels of Tyr oxidation products in oxidatively damaged proteins are associated with various diseases, including atherosclerosis [1], eye cataracts [2], Parkinson's, and Alzheimer's diseases [3]. As a result, clinical interest in Tyr oxidation products has led to the development of important techniques for their specific analysis.

First, providing a selective sample pretreatment or analyte conversion technique plays a significant role. Tyr-dependent oxidation studies have been achieved using several methods, including chemical, electrochemical, photochemical, and enzymatic oxidation with phenylalanine hydroxylase [4–7], as well as nonenzymatic oxidation by hydroxyl free radicals [8].

One of the most well-known enzymatic oxidation products of Tyr is L-DOPA (L-3,4-dihydroxyphenylalanine), catalyzed by the enzyme Tyr hydroxylase [9]. L-DOPA is a crucial intermediate in the biosynthesis of catecholamines, including dopamine, norepinephrine, and epinephrine, which play vital roles in neurotransmission and stress responses [10–12]. On the other hand, nonenzymatic oxidation of Tyr is often derived by reactive oxygen species (ROS) or metal ions, generating various quinones and reactive intermediates [4, 13, 14]. For instance, Tyr can be oxidized to form Tyr radicals, which may dimerize to produce di-Tyr, a cross-linked product commonly used as a biomarker for oxidative stress in proteins [15, 16]. Aromatic ring of Tyr can also be nitrated by peroxynitrite ($ONOO^-$). Superoxide ($O_2^{\bullet -}$) and nitrogen monoxide (•NO) combine quickly to generate $ONOO^-$ and it is suggested that the nitration of Tyr proceeds through a radical mechanism with the intermediary production of $\bullet NO_2$ [17]. Additionally, under strong oxidizing conditions, Tyr can degrade into smaller molecules such as *p*-hydroxyphenyl

pyruvic acid or homogentisic acid, which are involved in metabolic pathways or accumulate in certain genetic disorders like alkaptonuria [18, 19].

The oxidation products of Tyr have significant implications in both physiology and pathology. In melanocytes, the formation of melanin from Tyr oxidation protects cells from DNA damage [20]. While in neurodegenerative diseases like Parkinson's, this misregulation of Tyr-derived catecholamines contributes to neuronal degeneration [21]. Furthermore, oxidative modifications of Tyr residues in proteins are associated with aging, inflammation, and various diseases, highlighting the dual role of Tyr oxidation as both a protective mechanism and a contributor to oxidative damage [22, 23]. Understanding these pathways provides insights into therapeutic strategies targeting oxidative stress-related conditions [24].

Tyr-containing peptides are susceptible to oxidation, primarily through the modification of the phenolic side chain of Tyr residues. This oxidation can occur via various mechanisms, including reactions with ROS, metal-catalyzed oxidation, or enzymatic processes mediated by peroxidases or tyrosinases [4, 25, 26]. The primary oxidation products of Tyr include di-Tyr, DOPA, and Tyr quinones, which can lead to cross-linking or aggregation of peptides and proteins [13, 14, 25, 26]. Analytical techniques such as mass spectrometry and HPLC are commonly used to monitor Tyr oxidation products, enabling researchers to study their mechanisms and consequences. Understanding and controlling Tyr oxidation is crucial for optimizing peptide-based therapeutics, food products, and biomaterials [24, 27, 28].

Early electrochemical studies on Tyr confirmed its electroactive nature at carbon-based electrodes [29–32]. In 1980, Malfoy and Reynaud [29] reported the first mechanistic studies using gold and vitreous carbon electrodes. In a recent study, Todorov et al. [33] reported a more detailed mechanistic insight into tyrosine oxidation based on fast-scan cyclic voltammetry (CV) studies using carbon-fiber microelectrodes. They were able to distinguish between adsorbed and diffusing product species.

In 2010, Bischoff et al. [34] led a study on the electrochemical oxidation and cleavage of Tyr-containing peptides by coupling electrochemistry to mass spectrometry (EC–MS) as a potential instrumental alternative to chemical and enzymatic cleavage. The detected products were divided into three groups: cleavage products, noncleavage oxidation products, and unassigned products, which include dimers for Tyr-containing peptides.

Using EC, redox reactions can be easily achieved under physiologically relevant conditions. Electrochemical oxidation offers numerous benefits, including well-controlled parameters such as a wide variety of electrode materials, adjustable oxidation potentials, and variable reaction times, all within a simple setup [35]. Therefore, electrochemical oxidation is an attractive alternative to other oxidation processes.

Apart from sample pretreatment, several classical separation and detection techniques are available to analyze Tyr's oxidation products and understand the reaction mechanism. MS has become an important detection technique for the measurement of amino acids in recent years, which is usually coupled with GC or HPLC [36, 37].

In this context, coupling EC with MS (EC–MS) is among the most powerful techniques because it enables measurements to identify both products and intermediates of electrochemical reactions, although it requires significant expense and expertise [38]. Notably, the versatility of MS arises from two main points: first, MS is a highly sensitive and effective detector for electrochemical cells; second, its compatibility with many electrochemical setups and ability to provide information on molecular weight and isotopic patterns offer reliable data on various target analytes [39]. Additionally, MS analysis can contribute to structural determination using tandem MS techniques [40]. Overall, real-time coupling of EC with MS allows for the simultaneous characterization of both electrochemical and mass spectrometric properties of the analyte, delivering complementary information that improves understanding [41]. In this work, the EC–MS approach relies on the straightforward coupling of a modified electrochemical flow cell to an electrospray ionization (ESI) interface originally designed for capillary electrophoresis (CE) measurements [42].

CE is used as a separation method, and the oxidized sample is simply directly injected into the capillary from an integrated disposable screen-printed electrode surface [43]. This provides us with several advantages, such as easy coupling to MS, high-speed analysis, and efficient transfer into the separation system [43, 44].

In this study, a real-time mass voltammogram was recorded by online EC–MS using an electrochemical flow cell with an integrated disposable carbon screen-printed electrode, providing the potential-dependent product profile. On the other hand, EC–CE–MS electropherograms resulting from measurements with and without electrochemical pretreatment were investigated to study the separation behavior and the structural properties of the electrogenerated species.

2 | Experimental

2.1 | Chemicals and Materials

The following chemicals of analytical grade were used: acetic acid (Sigma–Aldrich, MO, USA), formic acid (Merck, Darmstadt, Germany), isopropanol (Roth, Karlsruhe, Germany), Tyr, caffeine, and 3-nitrotyrosine (Sigma–Aldrich, St. Louis, MO, USA). Fused silica capillaries (Polymicro Technologies, USA) with an inner diameter (ID) of 50 µm and an outer diameter (OD) of 360 µm were used. Disposable screen-printed carbon electrodes (SPCEs) (type DRP-110) were obtained from DropSens (Metrohm DropSens, Spain).

2.2 | EC–MS Experimental Setup

The electrochemical conversion of Tyr was performed using a modified flow cell (Metrohm DropSens, Spain) for screen-printed electrodes (SPEs). Type DRP110 SPEs (Metrohm DropSens, Spain) with carbon-based counter and working electrodes, and a silver quasireference electrode were used for all the

electrochemical protocols. All potentials refer to the silver quasireference electrode. A scan of potential was applied using a μAutolab III potentiostat, controlled by NOVA 2.0 software (Metrohm Autolab B. V., Utrecht, The Netherlands). The sample solution flowed through the electrochemical flow cell by implementing a syringe pump of type UMP3 with a Micro2T pump controller (World Precision Instruments, USA) equipped with a 1 mL glass syringe. For MS detection, a Bruker micrOTOF mass spectrometer (Bruker Daltonics, Bremen, Germany), equipped with a grounded coaxial sheath liquid ESI interface (Agilent Technologies, Waldbronn, Germany), was used. Sheath liquid (isopropanol/H_2O/formic acid 49.9:49.9:0.2 v/v/v) was injected using a syringe pump (Type 161 553, KD Scientific, Holliston, MA, USA), equipped with a 1 mL glass syringe (ILS, Stu·tzerbach, Germany) at a flow rate of 8 μL min^{-1}. A fused silica capillary (ID 50 μm) with a length of 21 cm was used to connect the flow cell and the MS. One side of the fused silica capillary (injection end) is polished with a 15-degree angle to keep the closest (and well-specified) distance between the tip of the capillary and the surface of the working electrode, and the detection end of the capillary is installed in a grounded ESI sprayer. The ESI–MS was operated in positive ion mode using the following settings: ESI voltage of 3 kV, mass range m/z 50–500, spectra rate 5 Hz, nebulizer 1.0 bar, dry gas 8.0 L min^{-1}, dry temperature 250°C.

2.3 | EC–CE–MS Experimental Setup

An existing fully automated EAI cell setup [43], in combination with a laboratory-assembled CE system and a micrOTOF-MS, was utilized to perform all experiments, as illustrated in Figure 1; 65 μL of the sample solution was applied to the central region of the SPE (DRP-110). During electrochemical pretreatment, a 1.2 V oxidation potential was applied for 20 s. Afterward, the separation capillary was automatically moved into the sample drop with an injection time of 10 s. The capillary was then moved back into the buffer vial. Electrophoretic separations were performed by applying a high voltage of 25 kV for all measurements. The separation capillaries were 35 cm long. The sample solution contained 1.0 mM Tyr and 0.05 mM caffeine as the electroosmotic flow (EOF) marker in 50 mM ammonium acetate (pH 7). 500 mM acetic acid with pH 3.6 was used as the buffer for the separation. MS/MS measurements were carried out using EC–CE combined with a Q-TOF-MS system (model 6540, Agilent Technologies) using the following parameters: ion source: AJS ESI; dry gas temperature 300°C; dry gas flow 8 L min^{-1}; nebulizer gas pressure 2.8 bar; sheath gas temperature 300°C; sheath gas flow 10 L min^{-1}. Collision-induced dissociation of target species at 10 and 20 eV.

3 | Results and Discussion

3.1 | Online EC–MS Measurements

To begin, CV measurements were performed to investigate the electrochemical activity of Tyr on SPE DRP-110. Figure 2 shows

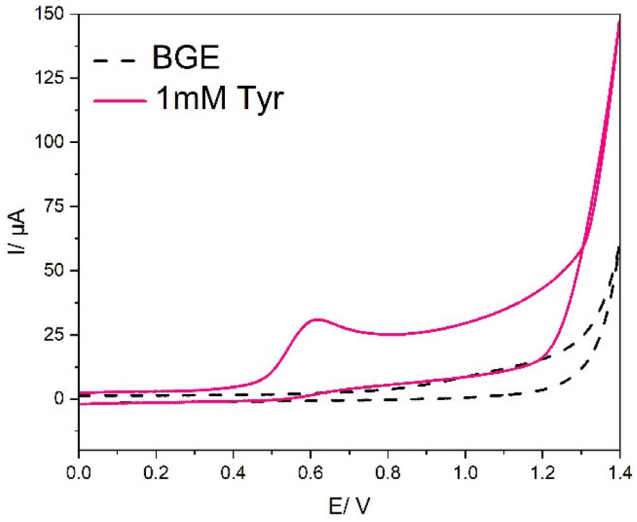

FIGURE 2 | Cyclic voltammograms of 50 mM ammonium acetate buffer (pH 7.2) as the background electrolyte (BGE) (black dashed line) and 1 mM Tyr in 50 mM BGE (pink line). Voltammograms were recorded from 0 to 1.4 V at a scan rate of 10 mV/s using SPCE DRP-110.

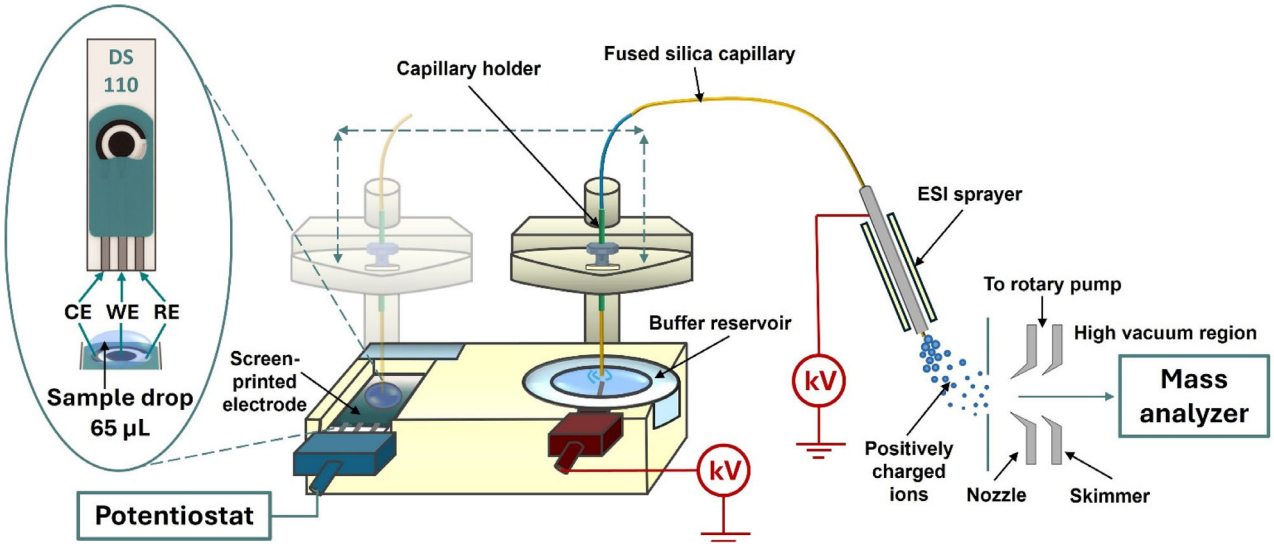

FIGURE 1 | Experimental setup of the fully automated EAI–CE–MS system.

the CV measurements of a 50 mM ammonium acetate buffer, pH 7.2, as the background electrolyte (BGE) and 1 mM Tyr prepared in BGE.

For the first step of our experiments, EC–MS measurements were carried out to gain information about the potential-dependent formation of electrogenerated oxidation products of Tyr. The sample solution was degassed using a sonication bath to release trapped gases, particularly oxygen, carbon dioxide, and nitrogen from the sample solution. To prevent the time delay between the electrochemical reaction and MS detection, the flow rate is optimized and set to 16 µL/min. This condition provides measurements with a transfer time of less than 2 s and makes it more probable to determine the less stable products, aside from the stable ones. Figure 3 shows the mass voltammogram of a 1 mM Tyr solution in 50 mM ammonium acetate in neutral media. A mass voltammogram not only validates MS information (m/z, MS signal intensity) but also allows for current-potential characteristics to be carried out at the same time. A different oxidation potential of Tyr in LSV measurements compared to CV measurements could be seen here as a result of the hydrodynamic nature of LSV measurements in a flow cell, providing a different mass transport situation. However, the CV measurement is done in static mode, outside of a flow cell.

Here, m/z indicates mass-to-charge ratios of protonated species ($[M+H]^+$). As can be seen, after 0.5 V, the intensity of the extracted ion trace of Tyr (m/z 182.08) decreases, and the mass intensity of the main electrochemical oxidation product, P1 (m/z 180.06), increases and stays almost the same until the end of the measurement. The mentioned product could be formed by a 2-electron transfer mechanism resulting in the keto–enol derivative of Tyr [33, 34].

At the potential range of 0.6 –1.1 V, one electron from the phenolic hydroxyl group is removed, generating a reactive Tyr phenoxyl radical. This radical undergoes dimerization to form di-Tyr, a stable cross-linked product. The extracted ion trace of 361.14 (P2) probably indicates dimerized Tyr [45]. The mass accuracy of the detected species was measured to be between 2 and 5 ppm. Another oxidation product, with a mass-to-charge ratio of 227.06 (P3), shows up in the potential range between 0.6 and 0.9 V. P3 could be generated through the addition of a nitrogen dioxide group ($\bullet NO_2$) to the phenolic ring, resulting in 3-nitrotyrosine. This is probably a result of complex electrochemical reactions happening on the surface of the electrode [33]. The very same results were achieved by measuring 1 mM tyrosine in 500 mM acetic acid, pH 3, to confirm that the formation of P3 is not an artificial effect of the used BGE. Through these measurement results, it can be seen that several species are being formed simultaneously, and many complex electrochemical processes are going on at the same time.

To the best of our knowledge, no online EC–MS studies were conducted on Tyr using SPEs, while several studies were conducted on the electrochemical oxidation of Tyr-containing peptides using a porous graphite electrode. Various oxidation products were reported, including peptide fragments formed by hydrolysis at the C-terminal side of Tyr [34, 46].

The low signal intensities in the EC–MS studies make it difficult to further investigate the details. Therefore, EC–CE–MS measurements were conducted by applying a specified potential for a longer timescale to not only determine migration behavior but also provide measurements with more detailed information.

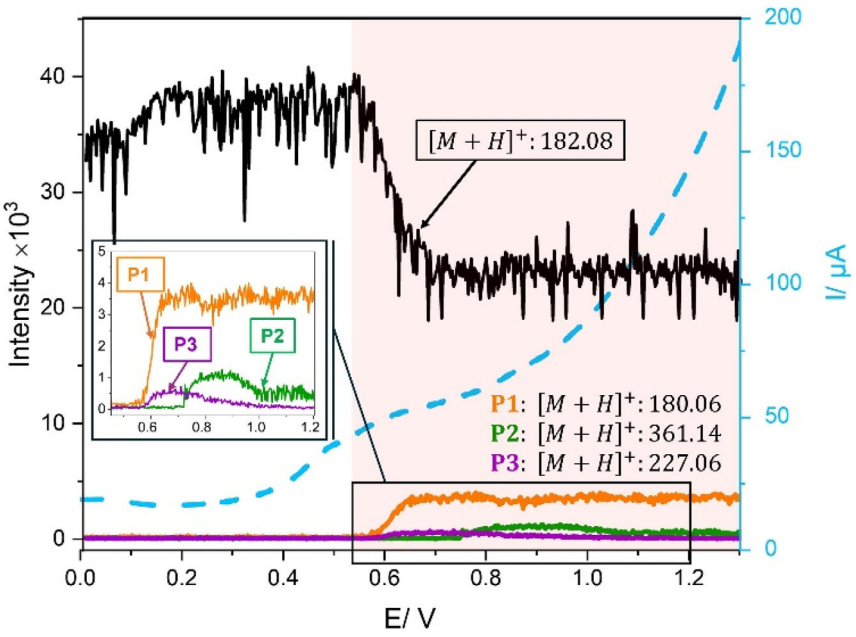

FIGURE 3 | Mass voltammogram of 1 mM Tyr solution in 50 mM ammonium acetate buffer (pH 7.2). The measurements were conducted on a carbon-based SPE implemented in a flow cell. Linear sweep voltammograms were performed from 0 to 1.3 V at a scan rate of 10 mV/s. Currents recorded during measurements are shown as a blue dashed line. The flow rate of the sample solutions was 16 µL/min. The transfer capillary had an ID of 50 µm and a length of 23 cm.

3.2 | EC–CE–MS Measurement

In the second part of the experiments, online EC–CE–MS measurements were performed on a 1 mM Tyr solution in 50 mM ammonium acetate adjusted to pH 7, containing 0.1 mM caffeine as an EOF marker. If the detected species in EC–MS measurements are unstable or prone to react while moving through the capillary, they may not be detected due to the longer transfer times through a rather long capillary in the CE part. Nevertheless, all the components detected in EC–MS measurements were stable enough to be detected in our EC–CE–MS configuration.

Using EC–CE–MS, the migration behavior and isotopic patterns of each compound detected by EC–MS measurements could be further studied to provide a seal of approval for the results of the previous measurement.

Figure 4 shows the electropherograms resulting from a measurement without electrochemical pretreatment (Figure 4A) and with applying electrochemical pretreatment (Figure 4B). The electrochemical pretreatment was performed through the following protocol: a potential of 1.2 V was applied for 20 s to 65 µL of 1 mM Tyr solution in 50 mM ammonium acetate adjusted to pH 7.0. The hydrodynamic injection lasted for 10 s using a fused silica capillary with an ID of 50 µm and a length of 35 cm. A 500 mM acetic acid solution with a pH value of 3.6 was used as the separation buffer, and the applied separation voltage was 20 kV. Observing the migration behavior shows that all the species migrate before the EOF marker.

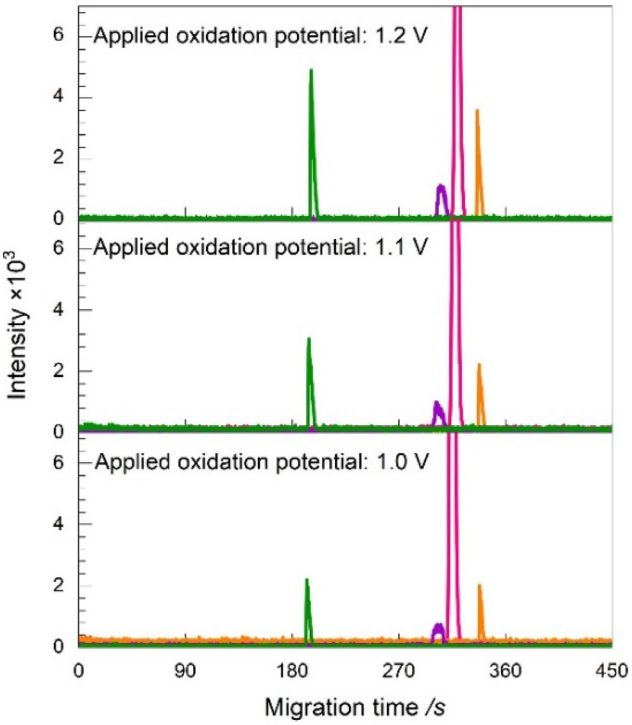

FIGURE 5 | Enlarged potential-dependent electropherograms of a 1 mM Tyr solution (pH 7, 50 mM ammonium acetate). The potential was applied for 20 s. Hydrodynamic injection lasted 10 s. The separation capillary had an ID of 50 µm and a length of 35 cm. The separation voltage was 20 kV, and the separation buffer was a 500 mM acetic acid solution, pH 3.6.

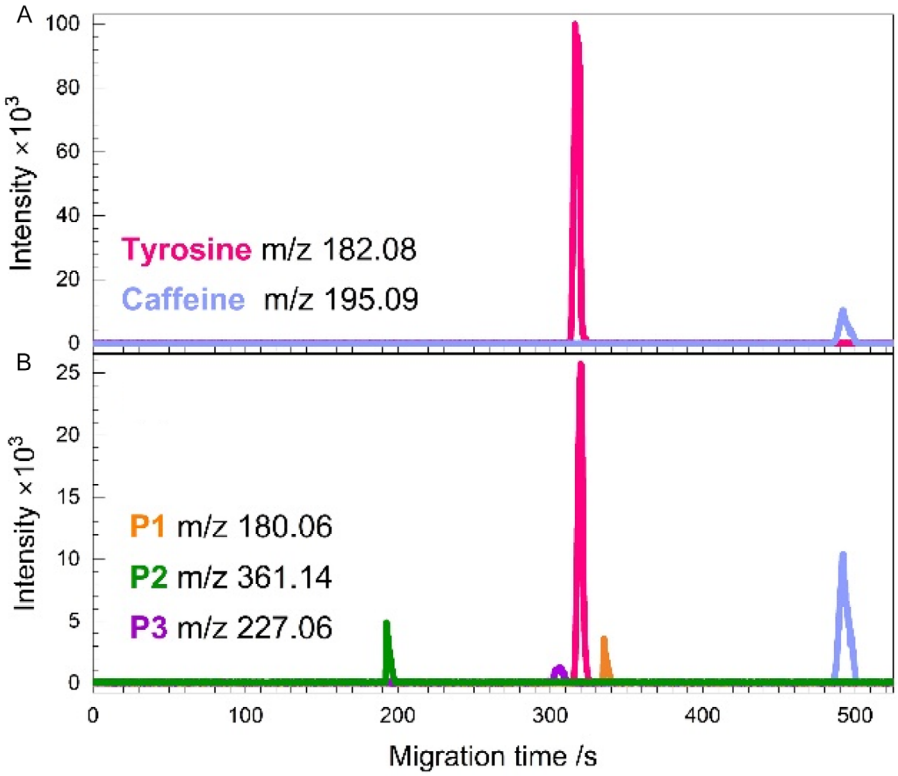

FIGURE 4 | Electropherograms for EC–CE–MS measurements without electrochemical pretreatment (A) and with an applied potential of 1.2 V (B). The potential was applied for 20 s. Hydrodynamic injection lasted 10 s. The separation capillary had an ID of 50 µm and a length of 35 cm. The separation voltage was 20 kV, and the separation buffer was a 500 mM acetic acid solution, pH 3.6.

This indicates that all the detected components moving in CE are positively charged (cationic). Without applying electrochemical pretreatment (Figure 4A), no signal related to the oxidation products was detected, while by applying electrochemical pretreatment (Figure 4B), four signals were recorded, each with a specific migration time. The extracted ion trace of Tyr (m/z 182.08) shows its specific migration time at 320 s, and the extracted ion trace related to P2 (m/z 361.14) shows up at 200 s. At 192 s, the mass trace of dimerized Tyr P2 (m/z 361.14) was recorded. The migration times of the other produced species with m/z ratios of 227.06 (P3) and 180.06 (P1) are at 305 and 335 s, respectively. The EC–CE–MS data show that not only does the major oxidation product (P1) form on the surface of SPE DRP-110 but also the two additional components that

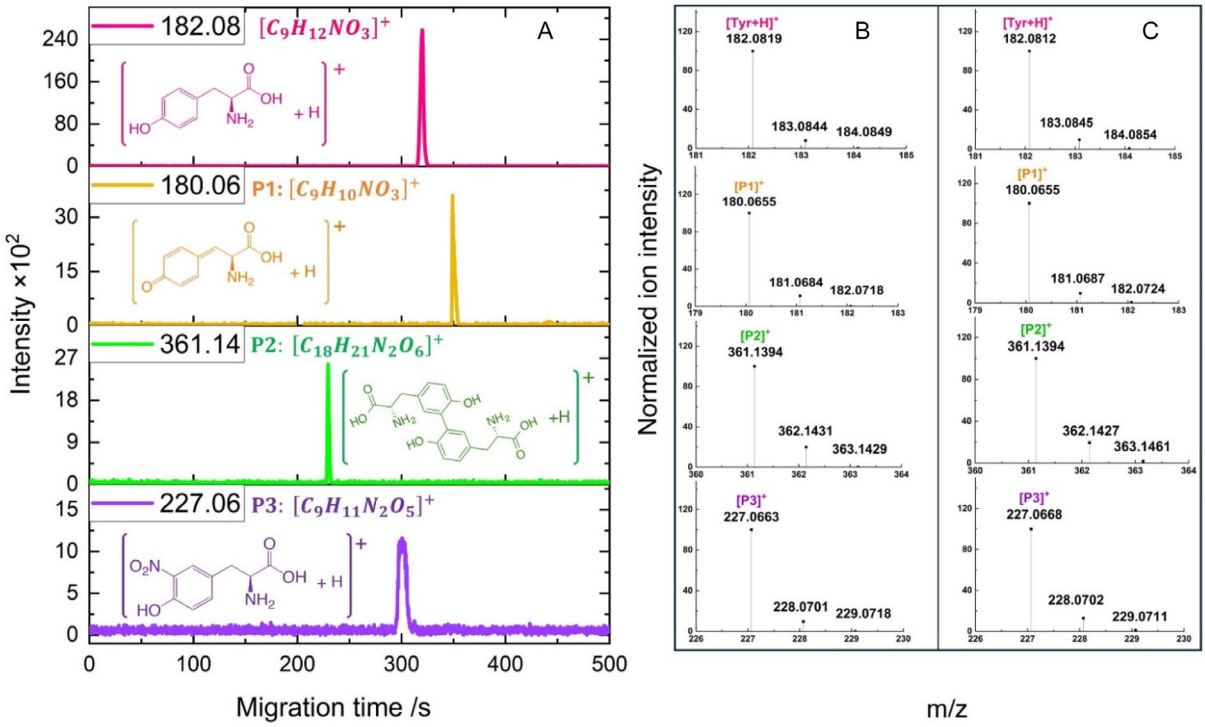

FIGURE 6 | EC–CE–MS Electropherograms (A) showing the specific migration times and suggested structures of each $[M+H]^+$, chemical formula, and structures. Normalized ion intensity versus m/z to show the measured (B) and the simulated (C) isotopic patterns.

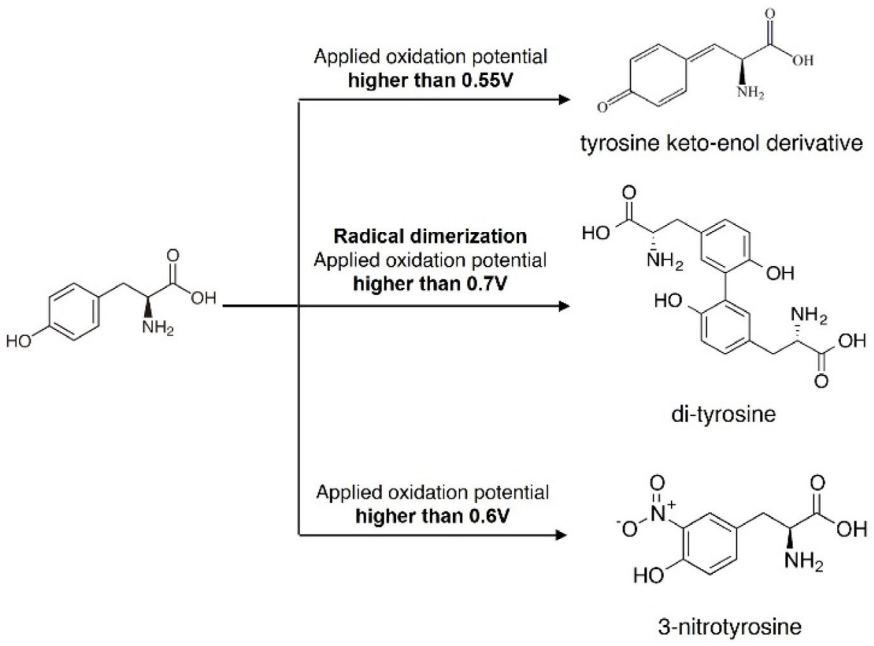

FIGURE 7 | Possible electrochemical mechanism for the formation of diffusive species during tyrosine oxidation on a SPE.

were observed in real-time EC–MS studies. This also provides results with sufficient signal intensities to further investigate the isotopic patterns.

To facilitate the understanding of the effect of the applied oxidation potential value in the electrochemical pretreatment protocol on the intensity of the detected species, Figure 5 is provided. The graph is enlarged due to the low intensities of the oxidation products; therefore, the intensity of Tyr is out of range.

Even though increasing the oxidation potential from 1.0 to 1.1 V and then to 1.2 V increases the intensity of the detected positively charged oxidation products, applying oxidation potentials lower than 1.0 V and higher than 1.2 V does not change the mass intensities. In mechanistic point of view, it can be concluded that, in some ways, adsorption is coupled with diffusion. Additionally, in the end, we are only able to detect species that are diffused into the solution.

Figure 6 illustrates the m/z ratios, migration times, and the simulated and measured isotopic patterns of positively charged Tyr and its electrogenerated products. These results enabled us to assign chemical formulas and propose possible structures. The found m/z ratio of 227.06 can be assigned to 3-nitrotyrosine, and this was confirmed by analyzing a standard solution of 3-nitrotyrosine regarding accurate mass determination, isotopic pattern, and migration time investigation.

To gain further mechanistic insight into the possible electrochemical oxidation of Tyr, Figure 7 summarizes the main results of this study.

4 | Conclusions

Reliable electrochemical modeling of Tyr oxidative stress has been studied in detail using CV, online EC–MS, and EC–CE–MS measurements, with a commercially available flow cell and a fully automated EAI-CE-MS system with an integrated commercial screen-printed electrode (SPE-DRP110). According to our studies, three main product species with positive ion traces of m/z of 180.06, 361.14, and 227.06 were found. A keto–enol derivative of Tyr, di-Tyr, and 3-nitrotyrosine were detected as the electrochemical oxidation products of Tyr. It is shown that hyphenating electrochemistry with mass spectrometry can be very beneficial toward reaching more in-depth and detailed studies on our target analyte in comparison with pure electrochemical approaches. This powerful approach to characterizing the redox products indicates that other oxidation products might be produced during electrochemical treatment of Tyr at even higher potentials, which are not detectable using classical methods. EC–MS and ECNCE–MS techniques emerge as powerful tools, thus making it possible to improve the understanding of reaction pathways through the identification of products or intermediates. It was clearly shown that various electrogenerated species are formed in voltametric experiments, simultaneously. However, in the context of our methodical approach, only diffusive product species can be recorded.

Acknowledgments

We would like to thank J. Feucht, J. Kiermaier, W. Söllner, and Dr. T. Herl for the measures concerning high-resolution mass spectrometry.

Open Access funding enabled and organized by Projekt DEAL.

Conflicts of Interest

The authors declare no conflicts of interest.

Data Availability Statement

The data that support the findings of this study are available from the corresponding author upon reasonable request.

References

1. J. Beckmann, Y. Ye, P. Anderson, et al., "Extensive Nitration Of Protein Tyrosines In Human Atherosclerosis Detected By Immunohistochemistry," *Biological Chemistry Hoppe-Seyler* 375 (1994): 81–88.

2. P. Antoinette, "Reaction of Tyrosine Oxidation Products with Proteins of the Lens," *The Biochemical Journal* 109 (1968): 301–305.

3. K. Barnham, F. Haeffner, G. Ciccotosto, et al., "Tyrosine Gated Electron Transfer Is Key to the Toxic Mechanism of Alzheimer's Disease β-amyloid," *The FASEB Journal* 18 (2004): 1427–1429.

4. F. E. Ali, K. J. Barnham, C. J. Barrow, and F. Separovic, "Metal Catalyzed Oxidation of Tyrosine Residues by Different Oxidation Systems of Copper/Hydrogen Peroxide," *Journal of Inorganic Biochemistry* 98 (2004): 173–184.

5. S. M. MacDonald and S. G. Roscoe, "Electrochemical Oxidation Reactions of Tyrosine, Tryptophan and Related Dipeptides," *Electrochimica Acta* 42 (1997): 1189–1200.

6. C. Giulivi, N. J. Traaseth, and K. J. A. Davies, "Tyrosine Oxidation Products: Analysis and Biological Relevance," *Journal of Amino Acids* 25 (2003): 227–232.

7. M. D. Davis and S. Kaufman, "Evidence for the Formation of the 4A-carbinolamine During the Tyrosine-dependent Oxidation of Tetrahydrobiopterin by Rat Liver Phenylalanine Hydroxylase," *The Journal of Biological Chemistry* 15 (1989): 8585–8596.

8. G. A. Molnár, E. Z. Mikolás, I. A. Szijártó, S. Kun, E. Sélley, and I. Wittmann, "Tyrosine Isomers and Hormonal Signaling: A Possible Role for the Hydroxyl Free Radical in Insulin Resistance," *World Journal of Diabetes* 6 (2015): 500–507.

9. P. J. Hillas and P. F. Fitzpatrick, "A Mechanism for Hydroxylation by Tyrosine Hydroxylase Based on Partitioning of Substituted Phenylalanines," *Biochemistry* 35 (1996): 6969–6975.

10. C. Schulz, G. Eisenhofer, and H. Lehnert, "Principles of Catecholamine Biosynthesis, Metabolism and Release," *Frontiers of Hormone Research* 31 (2004): 1–25.

11. C. M. Jin, Y. J. Yang, H. S. Huang, S. C. Lim, M. Kai, and M. K. Lee, "Induction of Dopamine Biosynthesis by l-DOPA in PC12 Cells: Implications of l-DOPA Influx and Cyclic AMP," *European Journal of Pharmacology* 591 (2008): 88–95.

12. L. Wecker and S. L. Ingram, *Brody's Human Pharmacology*, 7th Ed. (Elsevier, 2024), 137–142, ISBN. 9780323846738.

13. G. Woker and I. Antener, "Über Chinonreaktionen," *Helvetica Chimica Acta* 20 (1937): 1260–1270.

14. H. Eickhoff, G. Jung, and A. Rieker, "Oxidative Phenol Coupling—tyrosine Dimers and Libraries Containing Tyrosyl Peptide Dimers," *Tetrahedron* 57 (2001): 353–364.

15. E. P. L. Hunter, M. F. Desrosiers, and M. G. Simic, "The Effect of Oxygen, Antioxidants, and Superoxide Radical on Tyrosine Phenoxyl Radical Dimerization," *Free Radical Biology & Medicine* 6 (1989): 581–585.

16. T. DiMarco and C. Giulivi, "Current Analytical Methods for the Detection of Dityrosine, a Biomarker of Oxidative Stress, in Biological Samples," *Mass Spectrometry Reviews* 26 (2007): 108–120.

17. A. Vandervliet, J. P. Eiserich, C. A. Oneill, B. Halliwell, and C. E. Cross, "Tyrosine Modification by Reactive Nitrogen Species: A Closer Look," *Archives of Biochemistry and Biophysics* 319 (1995): 341–349.

18. C. David, A. Daro, E. Szalai, T. Atarhouch, and M. Mergeay, "Formation of Polymeric Pigments in the Presence of Bacteria and Comparison with Chemical Oxidative Coupling—II. Catabolism of Tyrosine and Hydroxyphenylacetic Acid by Alcaligenes Eutrophus CH34 and Mutants," *European Polymer Journal* 32 (1996): 669–679.

19. B. P. Norman, A. S. Davison, J. H. Hughes, et al., "Metabolomic Studies in the Inborn Error of Metabolism Alkaptonuria Reveal New Biotransformations in Tyrosine Metabolism," *Genes & Diseases* 9 (2022): 1129–1142.

20. M. Emanuelli, D. Sartini, E. Molinelli, et al., "The Double-Edged Sword of Oxidative Stress in Skin Damage and Melanoma: From Physiopathology to Therapeutical Approaches," *Antioxidants* 11 (2022): 612.

21. A. Napolitano, P. Manini, and M. d'Ischia, "Oxidation Chemistry of Catecholamines and Neuronal Degeneration: An Update," *Current Medicinal Chemistry* 18 (2011): 1832–1845.

22. N. Ogata, "Denaturation of Protein by Chlorine Dioxide: Oxidative Modification of Tryptophan and Tyrosine Residues," *Biochemistry* 46 (2007): 4898–4911.

23. S. Zhang, L. M. D. L. Rodriguez, F. F. Li, and M. A. Brimble, "Recent Developments in the Cleavage, Functionalization, and Conjugation of Proteins and Peptides at Tyrosine Residues," *Chemical Science* 14 (2023): 7782–7817.

24. X. Wu, M. Xu, M. Geng, et al., "Targeting Protein Modifications in Metabolic Diseases: Molecular Mechanisms and Targeted Therapies," *Signal Transduction and Targeted Therapy* 8 (2023): 220.

25. G. Oudgenoeg, R. Hilhorst, S. R. Piersma, et al., "Peroxidase-Mediated Cross-Linking of a Tyrosine-Containing Peptide with Ferulic Acid," *Journal of Agricultural and Food Chemistry* 49 (2001): 2503–2510.

26. R. Xiaokang, L. Zhao, C. Yuan, M. Shi, R. Xing, and X. Yan, "Enzyme-driven Oxygen-fuelled Pathway Selectivity Of Tyrosine-containing Peptide Oxidation Evolution," *Chemical Engineering Journal* 450 (2022): 138293.

27. M. Hellwig, "The Chemistry of Protein Oxidation in Food," *Angewandte Chemie International Edition* 58 (2019): 16742–16763.

28. P. Bhatt, S. G. Prajakta, V. V. S. P. K. Rayala, P. Radhakrishnanand, and K. Sankaranarayanan, "Non-Thermal Plasma Modulated l -Tyrosine Self-Assemblies: A Potential Avenue for Fabrication of Supramolecular Self-Assembled Biomaterials," *RSC Advances* 14 (2024): 13984–13996.

29. B. Malfoy and J. A. Reynaud, "Electrochemical Investigations of Amino Acids at Solid Electrodes," *Journal of Electroanalytical Chemistry and Interfacial Electrochemistry* 114 (1980): 213–223.

30. S. Karimi and M. Heydari, "Voltammetric Mixture Analysis of Tyrosine and Tryptophan Using Carbon Paste Electrode Modified by Newly Synthesized Mesoporous Silica Nanoparticles and Clustering of Variable-Partial Least Square: Efficient Strategy for Template Extraction in Mesoporous Silica Nanoparticle Synthesis," *Sensors and Actuators B: Chemical* 257 (2018): 1134–1142.

31. D. L. Sparks and J. T. Slevin, "Determination of Tyrosine, Tryptophan and Their Metabolic Derivitives by Liquid Chromatography-Electrochemical Detection: Application to Post Mortem Samples from Patients with Parkinson's and Alzheimer's Disease," *Life Science Journal* 36 (1985): 449–457.

32. X. Yu, Z. Mai, Y. Xiao, and X. Zou, "Electrochemical Behavior and Determination of L -Tyrosine at Single-walled Carbon Nanotubes Modified Glassy Carbon Electrode," *Electroanalysis* 20, no. 11 (2008): 1246–1251.

33. J. Todorov, G. S. McCarty, and L. A. Sombers, "Mechanistic Insight into Tyrosine Oxidation at Carbon-Fiber Microelectrodes Revealed by Fast-Scan Cyclic Voltammetry," *ACS Electrochemistry* 1, no. 8 (2025): 1423–1433.

34. J. Roeser, H. P. Permentier, A. P. Bruins, and R. Bischoff, "Electrochemical Oxidation and Cleavage of Tyrosine- and Tryptophan-Containing Tripeptides," *Analytical Chemistry* 82 (2010): 7556–7565.

35. G. Voravich and A. P. Trzcinski, "Removal of Pharmaceutically Active Compounds from Wastewater Using Adsorption Coupled with Electrochemical Oxidation Technology: A Critical Review," *Journal of Industrial and Engineering Chemistry* 126 (2023): 20–35.

36. W. M. Winnik and K. T. Kitchin, "Measurement of Oxidative Stress Parameters Using Liquid Chromatography–tandem Mass Spectroscopy (LC–MS/MS)," *Toxicology and Applied Pharmacology* 233 (2008): 100–106.

37. M. D. Zolodz, J. Minghong, L. Huiping, G. N. Henderson, and P. W. Stacpoole, "A GC–MS/MS Method for the Quantitative Analysis of Low Levels of the Tyrosine Metabolites Maleylacetone, Succinylacetone, and the Tyrosine Metabolism Inhibitor Dichloroacetate in Biological Fluids and Tissues," *Journal of Chromatography B* 837 (2006): 125–132.

38. T. Herl and F. M. Matysik, "Recent Developments in Electrochemistry–Mass Spectrometry," *ChemElectroChem* 7 (2020): 2498–2512.

39. J. Eidenschink, S. E. Bagherimetkazini, and F. M. Matysik, "Investigation of the Electrochemical Behavior of Cysteine by Hyphenation of Electrochemistry and Mass Spectrometry," *Monatshefte für Chemie - Chemical Monthly* 153 (2022): 775–780.

40. F. Lermyte, D. Valkenborg, J. A. Loo, and F. Sobott, "Radical Solutions: Principles and Application of Electron-based Dissociation in Mass Spectrometry-based Analysis of Protein Structure," *Mass Spectrometry Reviews* 37 (2018): 750–771.

41. P. Liu, M. Lu, Q. Zheng, Y. Zhang, H. D. Dewald, and H. Chen, "Recent Advances of Electrochemical Mass Spectrometry," *The Analyst* 138 (2013): 5519–5539.

42. T. Herl and F. M. Matysik, "Characterization of Electrochemical Flow Cell Configurations with Implemented Disposable Electrodes for the Direct Coupling to Mass Spectrometry," *Technisches Messen* 84 (2017): 672–682.

43. P. Palatzky, A. Zöpfl, T. Hirsch, and F. M. Matysik, "Electrochemically Assisted Injection in Combination with Capillary Electrophoresis-Mass Spectrometry (EAI-CE-MS) – Mechanistic and Quantitative Studies of the Reduction of 4-Nitrotoluene at Various Carbon-Based Screen-Printed Electrodes," *Electroanalysis* 25 (2013): 117–122.

44. T. Herl and F. M. Matysik, "Investigation of the Electrooxidation of Thymine on Screen-Printed Carbon Electrodes by Hyphenation of Electrochemistry and Mass Spectrometry," *Analytical Chemistry* 92 (2020): 6374–6381.

45. J. D. Figueroa, A. M. Zárate, E. Fuentes-Lemus, M. J. Davies, and C. López-Alarcón, "Formation and Characterization of Crosslinks, including Tyr–Trp Species, on One Electron Oxidation of Free Tyr and Trp Residues by Carbonate Radical Anion," *RSC Advances* 10, no. 43 (2020): 25786–25800.

46. H. P. Permentier, U. Jurva, B. Barroso, and A. P. Bruins, "Electrochemical Oxidation and Cleavage of Peptides Analyzed with on-line Mass Spectrometric Detection," *Rapid Communications in Mass Spectrometry* 17 (2003): 1585–1592.